Analysis of 2D Via-less Artificial Magnetic Conductors Using a Cavity Model

#Yading Li [1], Karu P. Esselle [1]
[1]*Center for Electromagnetic and Antenna Engineering,*
Electronic Department, Macquarie University
Sydney NSW 2109, Australia.
liyd@ics.mq.edu.au, esselle@ics.mq.edu.au.

Abstract

A rigorous full-wave cavity model is developed for 2D via-less (i.e. uni-planar) metallic periodic structures, which may or may not have a PEC ground plane. This model considers all the homogeneous material blocks in these structures as coupled electromagnetic cavities. This coupled cavity problem is then solved using magnetic vector potential. The via-less artificial magnetic conductor (AMC) surfaces are analyzed using this cavity model and the wave reflection coefficients are calculated for normal incidence case. The results show good agreement with the full-wave HFSS simulation results. To confirm the accuracy of this method, we also compare the electric fields calculated using the cavity model and HFSS.

1. INTRODUCTION

Usually the resonant phenomena of AMC surfaces are analyzed using transmission line models. For example, Yang [1]et. al. considered the substrate as an admittance load to the unit metal patches, and Ying [2]et. al. considered that the wave propagates and is reflected under the metal patches along the polarization direction of the incident wave. These transmission line models can only approximately determine the AMC resonant frequencies. One cannot get the information at the other frequencies using these simple models.

In this paper, we investigate a cavity model for 2D via-less metallic periodic structures. We expand the field in each cavity in forms of periodic Bloch modes and determine mode coefficients by imposing field continuity in the aperture areas. This cavity model gives the clear understanding about how a 2D periodic structure behaves as a perfect magnetic conductor (PMC). The reflection coefficients and the field distributions calculated using this model are compared to the simulation results of HFSS. Good agreements have been found.

2. CAVITY MODEL

We only analyze a unit cell of the 2D periodic structure, shown in Fig. 1, and apply periodic boundary conditions on the four sides. The bottom surface is a PEC and the top surface is open. Along the x direction the lattice constant is a ; along the y direction the lattice constant is b .

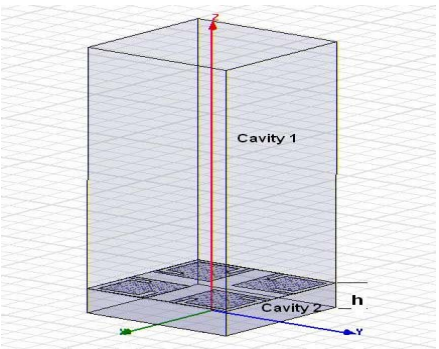

Fig. 1: Unit cell of a 2D via-less periodic structure. The shaded area is the metal patch. In this cavity model, the unit cell is divided into two cavities: Cavity 1 and Cavity 2

The shaded area represents the metal area of the unit cell and the gaps represent apertures or slots. We consider the problem as two cavities coupled by equivalent magnetic currents in the apertures of the metal layer. Using the equivalence theorem and aperture theory we separate the unit cell into two coupled cavities to solve the Maxwell Equations. Let us name them as Cavity 1 and Cavity 2 as shown in Fig. 1.

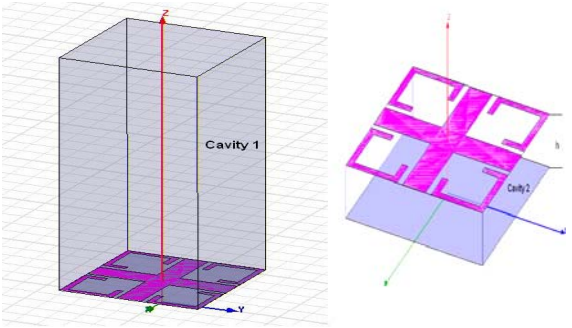

(a) (b)

Fig. 2: (a) Cavity 1 with open surface at top and PEC at bottom. Equivalent magnetic currents (shown in pink) exist just above the bottom PEC. (b) Cavity 2 with PEC surfaces at top and bottom. Equivalent magnetic currents (in pink) exist just below the top PEC.

In Cavity 1 (i.e. $z \geq h$) shown in Fig. 2(a), the top boundary condition is open, while the bottom boundary condition consists of equivalent magnetic currents just above the bottom

PEC. These equivalent magnetic currents exist in the area where the original structure (in Fig. 1) has apertures. There are two types of sources in this cavity: one is the incident wave $\vec{E}_i$ and the others are the equivalent magnetic currents $M_x = E_y^{tot}$ and $M_y = -E_x^{tot}$ appearing in the aperture areas of the unit cell. The total scattered field $\vec{E}^{tot}$ in Cavity 1 is $\vec{E}^{tot} = \vec{E}_r + \vec{E}_s$, where $\vec{E}_r$ is the reflected wave when an incident wave impinges on an infinite PEC surface and $\vec{E}_s$ is the electric field created by equivalent magnetic currents.

In Cavity 2 ($0 \le z \le h$) shown in Fig. 2(b), the top boundary condition consists of equivalent magnetic currents just below the top PEC. The bottom boundary is the PEC ground plane. There is only one type of source: the equivalent magnetic currents $M_x = -E_y^{tot}$ and $M_y = E_x^{tot}$ appearing in the aperture areas. Because there is a PEC ground plane in Cavity 2 at $z = 0$, the total scattered field is $\vec{E}^{tot} = \vec{E}_s$, where $\vec{E}_s$ are the electric field created by equivalent magnetic currents and their images formed by the two PEC surfaces.

To find $\vec{E}_s$ in Cavity 1 and Cavity 2, we need to solve Maxwell Equations in the "waveguide" bounded by two pairs of Bloch periodic boundaries, opened at the two ends and excited by equivalent magnetic surface currents and their images. We begin with the wave equations for magnetic vector potential $\vec{A}^m$ as follows:

$$\nabla^2 \vec{A}^m + k^2 \vec{A}^m = -\frac{\vec{M}}{j\omega\mu}\delta(z - z_p) \tag{1.1}$$

$$\vec{E} = -j\omega\mu\nabla \times \vec{A}^m \tag{1.2}$$

$$\vec{H} = \nabla \times \nabla \times \vec{A}^m \tag{1.3}$$

$$\vec{M}(x, y) = 2M_x\hat{x} + 2M_y\hat{y} \tag{1.4}$$

It is important to introduce the delta function into (1.1). Let $\vec{A}^m = A^{mx}\hat{x} + A^{my}\hat{y}$ and we get two scalar non-homogeneous wave equations:

$$\nabla^2 A^{mx} + k^2 A^{mx} = -\frac{2M_x}{j\omega\mu}\delta(z - z_p) \tag{2.1}$$

$$\nabla^2 A^{my} + k^2 A^{my} = -\frac{2M_y}{j\omega\mu}\delta(z - z_p) \tag{2.2}$$

The general solutions of equations (2.1) and (2.2), the non-homogeneous, second-order partial differential equations for 2D periodic structures, are:

$$A^{(1,2)my} = \sum_{m=-\infty}^{+\infty}\sum_{n=-\infty}^{+\infty} a_{mn}^{(1,2)y} FX(m)FY(n)FZ^{(1,2)}(m,n) \tag{3.1}$$

$$A^{(1,2)mx} = \sum_{m=-\infty}^{+\infty}\sum_{n=-\infty}^{+\infty} a_{mn}^{(1,2)x} FX(m)FY(n)FZ^{(1,2)}(m,n) \tag{3.2}$$

Here we notice that $FX(m)FY(n)$ are eigenmodes of hollow waveguides bounded by Bloch periodic boundary conditions. The sum of these modal functions, weighted with coefficients a_{mn}, gives the full-wave solution including both free and bounded waves or evanescent waves. To differentiate the solutions for Cavity 1 and Cavity 2, we use the superscripts (1,2) in equations (3.1) and (3.2). The superscript x, y represents the solutions excited by M_x or M_y. The superscript m represents the magnetic vector potential. The subscript mn represents the sequence of modal functions $FX(m)FY(n)$ given below. These modal functions are the same in Cavity 1 as in Cavity 2:

$$FX(m) = e^{-jk_m x}, \quad k_m = \frac{2m\pi + \phi_x}{a}$$

$$FY(n) = e^{-jk_n y}, \quad k_n = \frac{2n\pi + \phi_y}{b}$$

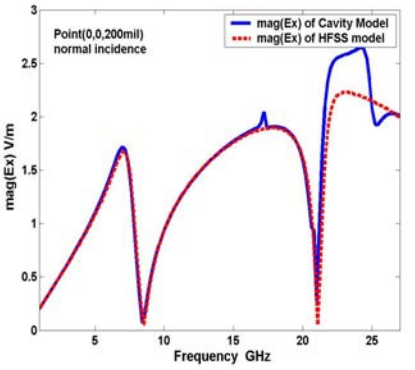

(a)

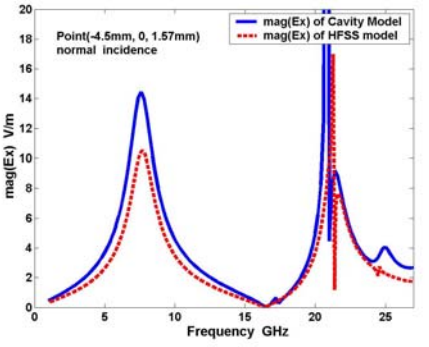

(b)

Fig.3: Electric field for the square patch AMC case in Table 1 calculated using the cavity model and HFSS. (a) Electric field at point (0,0,5.08mm) at 1GHz. (b) Electric field at point (-4.5,0,1.57mm) at 1GHz.

By imposing the continuity condition for electric and magnetic fields at the aperture area, we can derive a linear

system of equations for unknowns $a_{mn}^{(1,2)y}$ and $a_{mn}^{(1,2)x}$. We define

$$b_{mn}^{y} = a_{mn}^{(1)y}\left(-j\omega\mu\gamma_{mn}^{(1)}\right) = a_{mn}^{(2)y}\left(j\omega\mu\gamma_{mn}^{(2)}\right)$$

$$b_{mn}^{x} = a_{mn}^{(1)x}\left(j\omega\mu\gamma_{mn}^{(1)}\right) = a_{mn}^{(2)x}\left(-j\omega\mu\gamma_{mn}^{(2)}\right)$$

Through solving this linear system, we find the full wave solution for the 2D via-less, printed metallic periodic structure.

3. FIELD DISTRIBUTION

To confirm the accuracy of cavity model, the electric field calculated using the cavity model is compared to that obtained using HFSS for the square patch AMC surface listed in Table 1. We select two points one in the far field and the other at the aperture. Figs. 3(a) and (b) show good agreement for both far field and near field.

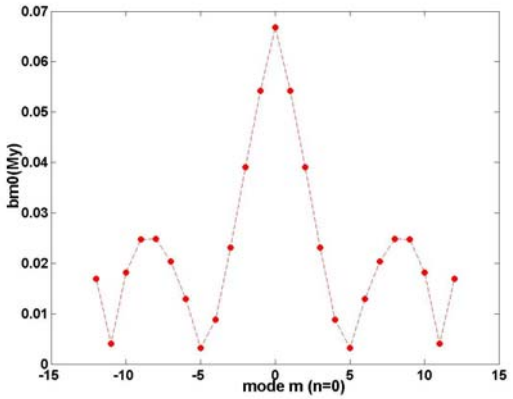

(a)

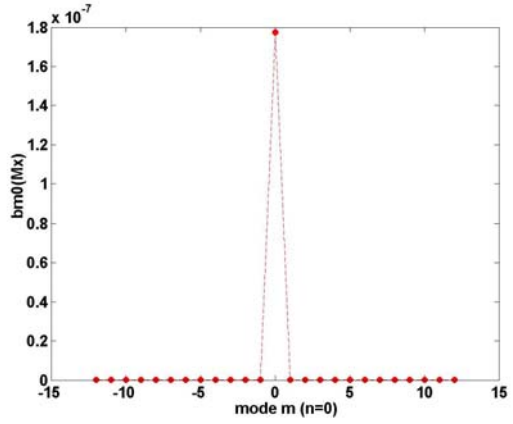

(b)

Fig.4: co-polar and cross-polar coefficients excited by an E_x -polarized normally incident wave. (a) Mode coefficient b_{m0}^{y}. (b) Mode coefficient b_{m0}^{x}.

Figs. 4(a) and (b) show the mode coefficients $b_{m0}^{(y)}$ and $b_{m0}^{(x)}$ of the same AMC, when a 1GHz E_x polarized plane wave is incident in normal direction. We do not expect cross polarization between E_x and E_y components in this case. This is indeed reflected in calculated coefficients shown in the Fig. 1: $b_{m0}^{(y)}$ is 0.07 and $b_{m0}^{(x)}$ is only 10^{-7}. This means any incident uniform plane wave $\left(H_{xi}, H_{yi}, H_{zi}\right) = \frac{1}{\omega\mu}\vec{k}_i \times (E_{xi}, E_{yi}, E_{zi})$ can be divided into two incident plane waves with E_{xi} and E_{yi} polarizations, given by $\left(H_{xi}^{y}, H_{yi}^{y}, H_{zi}^{y}\right) = \frac{1}{\omega\mu}\vec{k}_i \times (E_{xi}, 0, E_{zi}^{y})$ and $\left(H_{xi}^{x}, H_{yi}^{x}, H_{zi}^{x}\right) = \frac{1}{\omega\mu}\vec{k}_i \times \left(0, E_{yi}, E_{zi}^{x}\right)$ respectively. They excite M_y and M_x, respectively.

4. REFLECTION COEFFICIENT

To determine the wave reflection coefficient, we study $\vec{E}_s$ in detail in Cavity 1. When a x-polarized incident wave normally impinges on the AMC surface, only M_y is excited in the aperture. In this case

$$\vec{E}_s = E_r\hat{x} + E_x^{(1)y}\hat{x} = -E_i\hat{x} + E_x^{(1)y}\hat{x}.$$

where

$$E_x^{(1)y} = \sum_{m=-\infty}^{+\infty}\sum_{n=-\infty}^{+\infty} a_{mn}^{(1)y}\left(-j\omega\mu\gamma_{mn}^{(1)}\right) FX(m)FY(n)FZ_{\min}^{(1)}(m,n) = \sum_{m=-\infty}^{+\infty}\sum_{n=-\infty}^{+\infty} E_{xmn}^{(1)y} \quad (4)$$

When $m=0$ and $n=0$, $(\gamma_{00}^{(1)})^2 = \left(\frac{\phi_x}{a}\right)^2 + \left(\frac{\phi_y}{b}\right)^2 - (k^{(1)})^2$ is negative. The 00 mode in Cavity 1 is

$$E_{x00}^{(1)y} = -\frac{\int_{-\frac{a}{2}}^{\frac{a}{2}}\int_{-\frac{b}{2}}^{\frac{b}{2}} \vec{M}_y\, dxdy}{\Lambda} e^{-\gamma_{00}^{(1)}(z-h)} = b_{00}^{y} e^{-\gamma_{mn}^{(1)}(z-h)} \quad (5)$$

So this 00 mode is the propagating wave which satisfies $\theta_i = \theta_r$, where θ_i is the incident angle and θ_r is the reflected angle of the 00 mode. Besides the 00 mode, there can be a series of the other higher modes, which generally are evanescent modes when the frequency is low enough. With increasing of frequency, the higher modes may become propagating waves, but they do not satisfy $\theta_i = \theta_r$. So they are not ordinary reflected waves. Here we assure that only the 00 mode propagates. (This is the case with most AMC surfaces at the operating frequency.) Then, only $E_{x00}^{(1)y}$ contributes to the far field, and hence to the wave reflection coefficient. So the reflection coefficient R is:

$$R = \left(\frac{E_r + E_{x00}^{(1)y}}{E_i} \right)_{at \quad z=h} = \left(\frac{E_{x00}^{(1)y}}{E_i} - 1 \right)_{at \quad z=h} \qquad (6)$$

To further confirm the accuracy of this cavity model, we compare the phase angle of the reflection coefficients of three types of AMC surfaces using both the cavity model and HFSS. The parameters of these three AMC surfaces are in Table 1.

TABLE 1: PARAMETERS OF AMC SURFACES

Square patch AMC [2]	We select the same parameters as [2], except changing the size of the square metal patch to 8mm. $P = 10mm$, $W = L = 8mm$, $h_{subs} = 1.57mm$, $\varepsilon_r = 3.5$
UC-PBG [1]	We select the same parameters as [1]. $t = 25mil$, $a = 120mil$, $w = 10mil$, $d = 27.5mil$, $g = 10mil$, $g_1 = 20mil$. $\varepsilon_r = 10.2$.
Dual-band planar [4]	We select the same parameters as [4]. $a = 5mil$, $b = 40mil$, $c = 100mil$, $d = 120mil$, $e = 20mil$, $f = 27.5mil$, $h = 25mil$, $\varepsilon_r = 10.2$.

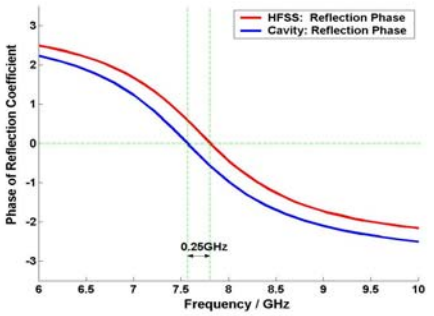

(a)

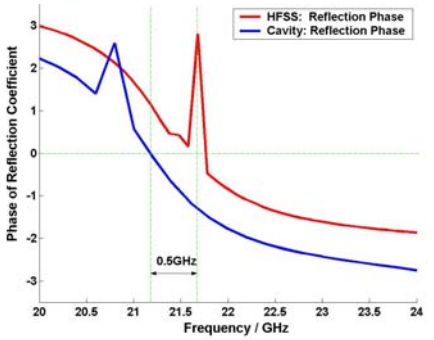

(b)

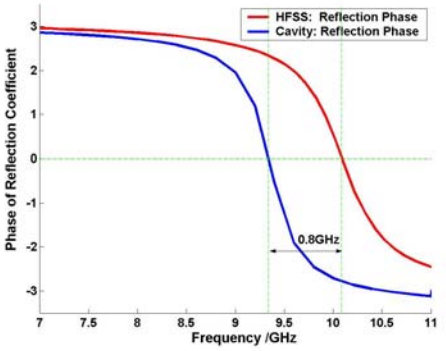

(c)

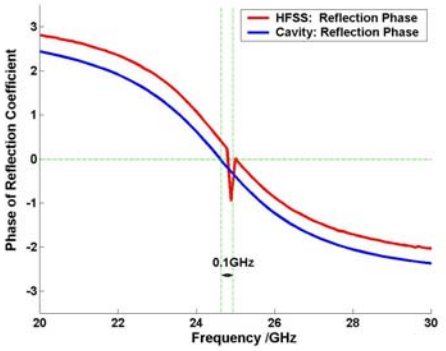

(d)

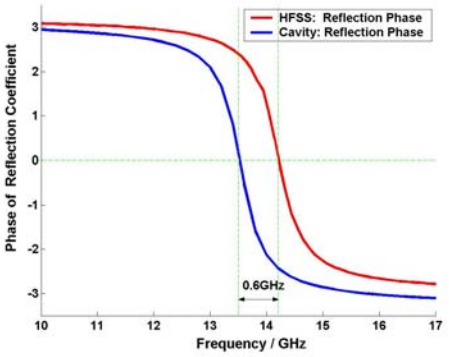

(e)

Fig.5: Reflection phase angle calculated using the cavity model and HFSS. (a) Square patch AMC lower band. (b) Square patch AMC upper band. (c) Dual-band planar AMC lower band. (d) Dual-band planar AMC upper band. (e) Single AMC band of UC-PBG

Using the cavity model, we calculate reflection phase based on equation (6). For the square patch AMC, the infinite series are truncated at $m, n \in [-15,...,0,...,15]$. For the other two AMC surfaces, the infinite series are truncated at $m, n \in [-20,...,0,...,20]$. In HFSS, we integrate E_x on a surface normal to z direction and average phase angle of the reflection coefficient in this area. Figs. 5(a)-(e) compare the results obtained using the cavity model with those obtained

using HFSS for several AMC bands of the three AMC surfaces listed in Table. 1

In general, we note a shift in frequency between two results. Depending on the surface and band, this shift is in the range of $0.4\% - 8.1\%$. Always the cavity model predicted a resonant frequency that is less than what is predicted by HFSS.

To test whether the AMC behaves as a perfect magnetic conductor (which has a reflection coefficient magnitude of unity in addition to zero phase), we also calculated the real and imaginary parts of the reflection coefficient using HFSS (based on equation (6)) and compared the results with those obtained using the cavity model. Figs. 6(a)-(b) show a good agreement between the two results.

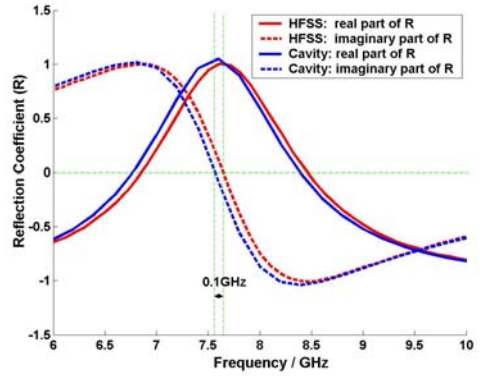

(a)

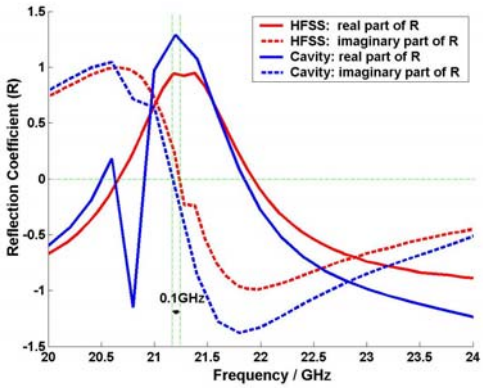

(b)

Fig.6: Real and imaginary parts of the reflection coefficient calculated using the cavity model and HFSS (based on equation (6)). (a) Lower band of square patch AMC. (b) Upper band of square patch AMC.

If the surface behaves as an AMC at a certain frequency, we naturally expect $R = 1 + j0$, i.e. $\frac{E_{x00}^{(1)y}}{E_i} = 2$ at $z = h$, the same as PMC boundary condition. As we expected the real part of R is close to 1 and imaginary part of R is near 0 at AMC frequencies in Figs. 6(a)-(b). In the end we understand that the AMC surface has the same propagating waves as PMC, which guarantees that the AMC behaves as a PMC in the far field. Of course, a PMC does not have evanescent waves like AMC. However it is just because of these evanescent modes around an AMC, a 2D periodic electric metallic structure can have the same far-field reflected wave as PMC.

Here we briefly consider frequency selective surfaces (FSS) to complete the discussion. As we know, an FSS can provide total reflection or total transmission properties. The total reflection includes in-phase ($\frac{E_{x00}^{(1)y}}{E_i} = 2, at \quad z = h$) and 180^o out-of-phase total reflection ($E_{x00}^{(1)y} = 0, at \quad z = h$). The total transmission occurs when it behaves as a matched load to the input source ($\frac{E_{x00}^{(1)y}}{E_i} = 1, at \quad z = h$).

5. CONCLUSION

A cavity model has been presented to analyze and understand the behaviour of 2D via-less (uni-planar) metallic periodic structures. It correctly describes both the far field and the near field of AMC surfaces. The wave reflection coefficients are calculated using the cavity model agree well with HFSS simulation results. This cavity model is general enough to analyze any 2D via-less periodic structures with or without PEC ground plane (including frequency selective surfaces). It can be extended to multi-layer printed EBG/FSS surfaces.

ACKNOWLEDGEMENT

The authors are thankful to Professor Tatsuo Itoh and Professor Yahya Rahmat-Samii for the valuable discussions when the first author visited University of California, Los Angeles, in 2005.

REFERENCES

[1] Fei-Ran Yang, Kuang-Ping Ma, Tatsuo Itoh, "A Novel TEM Waveguide Using Uniplanar Compact Photonic-Bandgap (UC-PBG) Structure.", *IEEE Trans. On Microwave Theory and Technologies.*, vol. 47 pp. 2092-2098, Nov. 1999.

[2] Ying Zhang, Jurgen von Hagen, Werner Wiesbeck, "Planar Artificial Magnetic Conductors and Patch Antennas", *IEEE Trans. On Antennas and Propagation.*, vol. 51, no. 10, pp. 2704-2712, Oct. 2003.

[3] B.AI-Jibouri, H Evans and E.korolkiewicz, "Cavity Model of circularly polarized cross-aperture-coupled microstrip antenna.", *IEE Proc.-Microwave Antennas Propag.* vol. 148, no.3, pp. 147-152, June. 2002.

[4] Yading Li, Karu P. Esselle, "Dual-Band Planar Compact Artificial Magnetic Conductor.", *IEEE APS. Symp. Washington, 2005.*

[5] R.M.Mateos, P. Ferrer, C. Craeva "Reactive Fields Above An Artificial PMC.", *IEEE APS. Symp. Washington 2005.*